Modeling cosmogenic radionuclides 10Be and 7Be during the Maunder Minimum using the ECHAM5-HAM General Circulation Model

U. Heikkilä, J. Beer, J. Feichter

Atmos. Chem. Phys., 8, 2797–2809, 2008
www.atmos-chem-phys.net/8/2797/2008/

Atmospheric Chemistry and Physics

Modeling cosmogenic radionuclides ^{10}Be and ^{7}Be during the Maunder Minimum using the ECHAM5-HAM General Circulation Model

U. Heikkilä[1], **J. Beer**[1], **and J. Feichter**[2]

[1]EAWAG, Dübendorf, Switzerland
[2]Max-Planck Institute for Meteorology, Hamburg, Germany

Received: 18 September 2007 – Published in Atmos. Chem. Phys. Discuss.: 1 November 2007
Revised: 4 March 2008 – Accepted: 9 May 2008 – Published: 29 May 2008

Abstract. All existing ^{10}Be records from Greenland and Antarctica show increasing concentrations during the Maunder Minimum period (MM), 1645–1715, when solar activity was very low and the climate was colder (little ice age). In detail, however, the ^{10}Be records deviate from each other. We investigate to what extent climatic changes influence the ^{10}Be measured in ice by modeling this period using the ECHAM5-HAM general circulation model. Production calculations show that during the MM the mean global ^{10}Be production was higher by 32% than at present due to lower solar activity. Our modeling shows that the zonally averaged modeled ^{10}Be deposition flux deviates by only ∼8% from the average increase of 32%, indicating that climatic effects are much smaller than the production change. Due to increased stratospheric production, the ^{10}Be content in the downward fluxes is larger during MM, leading to larger ^{10}Be deposition fluxes in the subtropics, where stratosphere-troposphere exchange (STE) is strongest. In polar regions the effect is small. In Greenland the deposition change depends on latitude and altitude. In Antarctica the change is larger in the east than in the west. We use the ^{10}Be/^{7}Be ratio to study changes in STE. We find larger change between 20° N–40° N during spring, pointing to a stronger STE in the Northern Hemisphere during MM. In the Southern Hemisphere the change is small. These findings indicate that climate changes do influence the ^{10}Be deposition fluxes, but not enough to significantly disturb the production signal. Climate-induced changes remain small, especially in polar regions.

Correspondence to: U. Heikkilä
(ulla.heikkilae@eawag.ch)

1 Introduction

^{10}Be (half-life 1.5 million years) and ^{7}Be (half-life 53.2 days) are natural radionuclides, which are produced in the atmosphere by collisions of cosmic ray particles with atmospheric N and O atoms. Their production rate anticorrelates with solar activity and the geomagnetic field intensity due to magnetic shielding of the cosmic rays by solar wind and the geomagnetic dipole field (Masarik and Beer, 1999). Soon after their production ^{10}Be and ^{7}Be become attached to ambient aerosols (mostly sulfate) and are transported and deposited with them. Besides radioactive decay the only sink for the radionuclides is wet and dry deposition. Owing to its long half-life, ^{10}Be can be measured in natural archives, revealing information about past changes in the production rate. ^{10}Be measured in ice cores has recently been used to reconstruct the solar activity during the Holocene (McCracken et al., 2004; Muscheler et al., 2007; Vonmoos et al., 2006). All these reconstructions are based on the assumption that the ^{10}Be concentrations archived in ice are directly proportional to the production rate. While this is a reasonable first assumption in view of the fact that ^{10}Be is well mixed during its residence time of 1–2 years in the stratosphere, and changes in snow accumulation rate are smoothed out when averaged over several years, climate changes lasting over decades, such as the cooling which occurred during the Maunder Minimum, could cause significant changes in the ^{10}Be concentrations in ice. Comparison of Arctic and Antarctic ^{10}Be records reveals very similar variability overall indicating that the variations observed are solar changes. However, in detail the records deviate from each other. Figure 1 shows the ^{10}Be concentrations measured in ice at four different sites, Dye3 (Beer et al., 1990) and Milcent (Beer et al., 1988a) in Greenland and Dome Concordia and the South Pole in Antarctica (Bard et al., 1997; Raisbeck et al., 1978;

Published by Copernicus Publications on behalf of the European Geosciences Union.

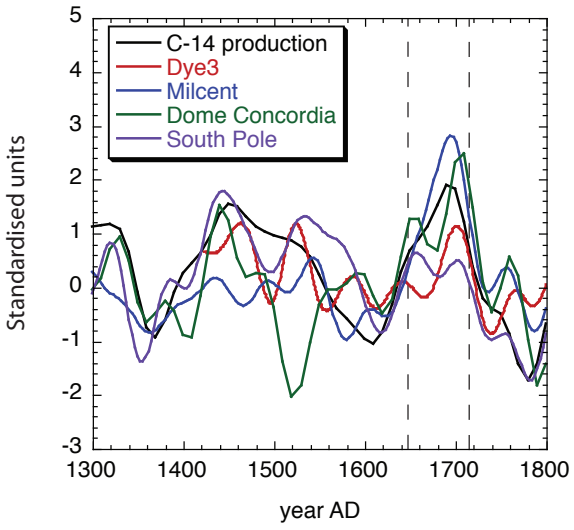

Fig. 1. ^{10}Be concentrations measured in ice at two Greenlandic stations (Dye3 (Beer et al., 1990) and Milcent (Beer et al., 1988a)) and two Antarctic stations (South Pole and Dome Concordia (Bard et al., 1997; Raisbeck et al., 1978; Raisbeck et al., 1990)) and the ^{14}C production rate derived from tree rings. The data has been standardized and filtered with a 50-year low-pass filter because of the different temporal resolution of the data.

Raisbeck et al., 1990). All records have been standardized, i.e. the mean value has been subtracted and the record is divided by the standard deviation. The production rate of another cosmogenic radionuclide, ^{14}C, is also shown (Stuiver et al., 1977). The production processes of ^{14}C are similar to those of ^{10}Be, but ^{14}C is archived in tree rings and its geochemical behavior is completely different. After its production ^{14}C oxidizes to $^{14}CO_2$ and is involved in the carbon cycle.

Although extracted from completely different types of archives situated in very different latitudes, both radionuclides show a similar production signal (Beer et al., 1988b, 1994). This is reflected in Fig. 1 by the fact that all data sets show a maximum during the Maunder Minimum, although its intensity varies. This indicates that the radionuclides show a common solar signal even though their concentrations are influenced by the local meteorology.

The Maunder Minimum (1645–1715) coincides with the coldest period during the Little Ice Age (1300–1800) in the Northern Hemisphere. This period is characterized by especially low solar activity, during which very few sunspots were observed. The change in the solar irradiance between the Maunder Minimum and the present day is not known and the estimates range from 0.05% to 0.5% (see Luterbacher (1999) and references therein for discussion). The Late Maunder Minimum (1675–1715) was the climax of this cold period with especially severe winters and wetter and colder summers in central and eastern Europe (Luterbacher, 1999).

In order to study production and climate related changes of ^{10}Be and ^{7}Be transport and deposition to polar regions during two climatically different periods, we compare the Maunder Minimum (MM) with Present Day (PD). The ^{10}Be concentrations measured in ice depend on the solar modulation of the production rate, the stratosphere-troposphere exchange (STE), the tropospheric transport and the precipitation rate at the measurement site. An important question is to what extent the production changes of ^{10}Be are masked by the meteorological conditions during periods of variable climate. Another interesting issue is whether there have been changes in the intensity of STE which can influence the ^{10}Be concentrations between MM and PD. Finally, we want to investigate whether climate induced changes in ^{10}Be deposition differ between Greenland and Antarctica.

An earlier general circulation model study has addressed the effect of a changing climate on ^{10}Be. Field et al. (2006) modeled the transport of ^{10}Be to polar regions under variable solar, magnetic field and greenhouse gas conditions. Their model simulations confirmed that changes in transport should be taken into account when inferring production changes in ice cores.

The ^{10}Be/^{7}Be ratio offers an interesting tool to study the stratospheric transport of the radionuclides. The ^{10}Be/^{7}Be ratio at the time of production is 0.5. Since this ratio only depends on the nuclear reactions, it can be considered as constant in time (Lal and Peters, 1967; Masarik and Beer, 1999). However, the ratio grows exponentially with time due to the radioactive decay of ^{7}Be. Koch and Rind (1998) and Rehfeld and Heimann (1995) have used the ^{10}Be/^{7}Be ratio in their model runs to study stratospheric transport. Land and Feichter (2003) also used the ^{10}Be/^{7}Be ratio to study the effect of a changing climate on the STE. They found that the induced changes in STE were latitude dependent depending on the involved processes. They concluded that the ^{10}Be/^{7}Be ratio depends not only on the STE but also on tropospheric transport in a changing climate which thus has to be taken into account.

The ^{10}Be/^{7}Be ratio has also been used in connection with observational data to detect STE. Heikkilä et al. (2008a) measured ^{10}Be and ^{7}Be at a high and a low altitude station in Switzerland and detected a maximum of ^{10}Be/^{7}Be in spring at the high altitude station. The ratio at the low altitude station did not show such a strong spring peak. Also Brown et al. (1988), Graham et al. (2003) and Monaghan et al. (1985/1986) have published ^{10}Be/^{7}Be ratios. Graham et al. (2003) also detected a maximum in the ^{10}Be/^{7}Be ratio during winter and spring. The ratios, all measured in the midlatitudes, vary between 1.3 and 2, which is higher than the global average of 1.1–1.4 estimated by (Heikkilä et al., 2008a) using a 2-box model pointing to a strong latitudinal dependence.

2 Model description and setup

ECHAM5 is a fifth-generation atmospheric global circulation model (GCM) developed at the Max-Planck Institute for Meteorology, Hamburg, evolving originally from the European Centre of Medium Range Weather Forecasts (ECWMF) spectral weather prediction model. It solves the prognostic equations for vorticity, divergence, surface pressure and temperature, expressed in terms of spherical harmonics with a triangular truncation. Non-linear processes and physical parametrizations are solved on a Gaussian grid. A complete description of the ECHAM5 GCM is given in Roeckner et al. (2003). The additional aerosol module HAM includes the microphysical processes, the emission and deposition of aerosols, a sulfur chemistry scheme and the radiative property scheme of the aerosols (Stier et al., 2005). For this study a model version with a horizontal resolution of T42 (2.8×2.8 degrees) with 31 vertical levels up to 10 hPa ($\sim$31 km) was used. Each run was allowed to spin up for five years to let ^{10}Be reach the equilibrium. For the MM, only the years 1705–1709, and for the PD, the years 1986–1990, were used for the analysis. The production rates of the radionuclides were taken from Masarik and Beer (1999). The profiles were interpolated as a function of latitude and altitude using the solar modulation function Φ available at http://www.faa.gov/education_research/research/med_humanfacs/aeromedical/radiobiology.

These Φ values differ only slightly from values reconstructed by Usoskin et al. (2005). For the PD run, monthly mean Φ values were used so that temporal changes in the production rate were taken into account by the model. During the MM a constant value of Φ=200 MeV was assumed, which is an average for the whole period of MM (McCracken et al., 2004). This increases the production rate of cosmogenic radionuclides by 32% during the MM compared with PD. The change in the geomagnetic field intensity is small and was neglected in this study (Yang et al., 2000).

The aerosol emission for both scenarios PD (year 2000) and MM (preindustrial, year 1750) was taken from the AEROCOM aerosol model inter-comparison experiment B. This data is available at http://nansen.ipsl.jussieu.fr/AEROCOM.

For these runs we used prescribed sea surface temperatures (SST), which were obtained from the coupled atmosphere-ocean model ECHAM4-HOPE-G (ECHO-G) run (Gonzalez-Rouco et al., 2003; Zorita et al., 2005). During the MM the solar constant was reduced by 1.5 W/m^2 compared with the present day value of 1365 W/m^2 following the ECHO-G run (Crowley et al., 2000). The greenhouse gases were set to preindustrial values (CO_2=283 ppm, CH_4=716 ppm, N_2O=276.7 ppm, CFCs=0). This leads to a reduction of the global mean temperature by 0.7 K during the MM.

A comparison with the observations shows a tendency of the simulations to underestimate observed deposition fluxes and atmospheric concentrations. Although observational data are sparse, this indicates that the source strength may be underestimated. The Masarik and Beer (1999) production rate was therefore increased by 50%. In their most recent production calculations the stratospheric production rate is higher by 15%, the tropospheric rate by 11 % and the global average production rate by 13% (Masarik, 2008[1]). Hence, the production increase of 50% made for this study represents rather an upper limit.

2.1 Deposition of ^{10}Be and ^{7}Be

The ^{10}Be and ^{7}Be are transported in ECHAM5-HAM similarly to aerosols. The deposition of these tracers, however, needs to be described explicitly because the deposition processes of the aerosol module HAM depend on the aerosol characteristics, such as solubility and size. It is necessary to define to which aerosols ^{10}Be and ^{7}Be are attached and to describe their deposition proportional to these aerosols. This appeared to be the most important issue in modeling the radionuclides. Since most of the radionuclides are produced in the stratosphere (50% according to Masarik and Beer (1999) and 67% according to Lal and Peters (1967)) where sulfate particles dominate, a strong connection between sulfate and ^{7}Be deposition has been established (Igarashi et al., 1998) and ^{10}Be and ^{7}Be were only attached to sulfate.

ECHAM5-HAM calculates the sedimentation and dry deposition as a product of the sedimentation or dry deposition velocity and the atmospheric aerosol concentration. The sedimentation is calculated throughout the atmospheric column. The dry deposition depends on the aerodynamic resistance of the surface and acts as a lower boundary condition for the vertical diffusion. Therefore it is only calculated for the surface layer concentration. For the radionuclides the sedimentation velocity and dry deposition velocity are calculated as an average of the deposition velocities of the aerosols. This average is weighted by the surface area of the aerosols because the probability of a radionuclide becoming attached to an aerosol is proportional to its surface area.

The wet deposition of aerosols in ECHAM5-HAM is treated differently for convective and stratiform clouds. A wet scavenging efficiency is calculated by both the convective and the stratiform routines and averaged. The averaged scavenging efficiency is then applied to the wet deposition of the radionuclides.

In ice clouds we assume that only 10% of the radionuclide mass is scavenged by nucleation scavenging (Feichter et al., 2004).

[1] Masarik, J. and Beer, J.: Simulation of particle fluxes and cosmogenic nuclide production in the Earth's atmosphere revisited, J. Geophys. Res., submitted, 2008.

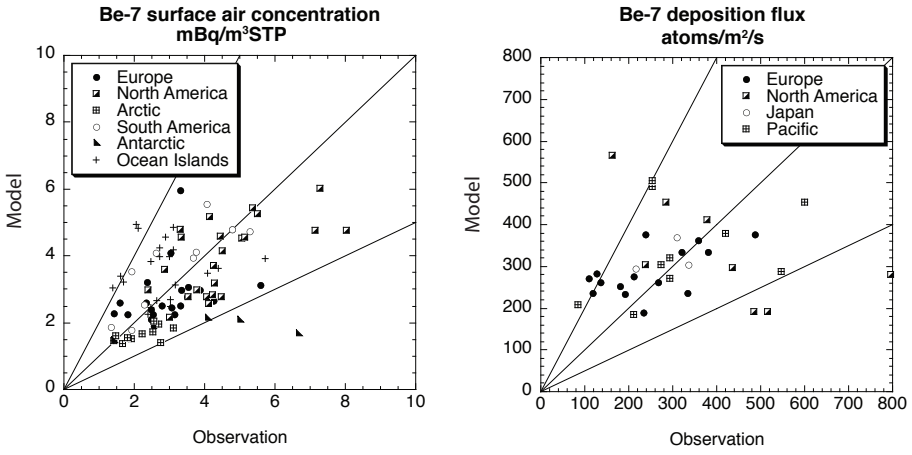

Fig. 2. Scatter plot of modeled and observed ^{7}Be surface air concentrations (91 stations) and deposition fluxes (36 stations). Almost all modeled values are within the factor of 2 of the observed values (straight lines).

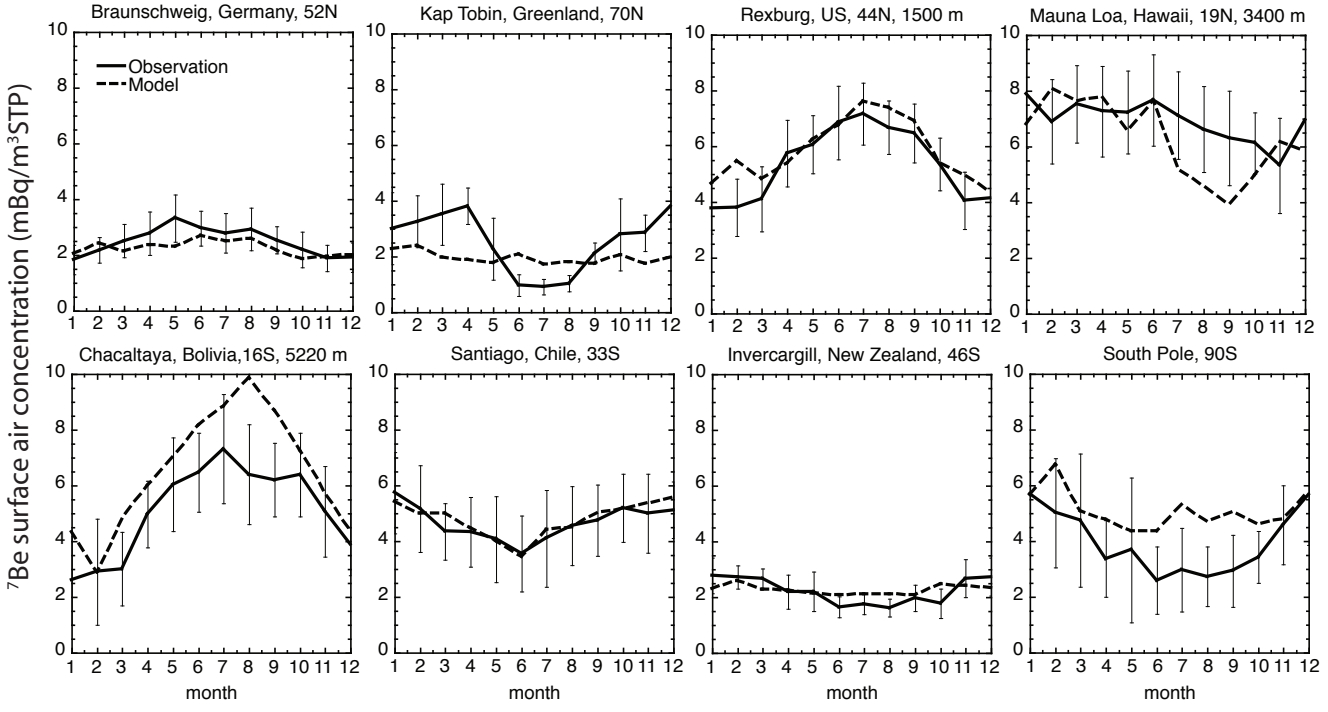

Fig. 3. Seasonal cycles of ^{7}Be measured (full line) in surface air (mBq/m^{3}STP) at selected stations worldwide compared with the modeled (dashed line) concentrations. The error bars show the standard deviations of the monthly averages of the different years (8–30 years depending on the station).

3 Model validation

3.1 Surface air concentrations and deposition fluxes

To validate the modeled ^{7}Be surface air concentrations, the collection of ^{7}Be data measured in air filters worldwide, provided by the Environmental Measurement Laboratory, has been used. Yearly average concentrations are available for 91 stations, and seasonal data for 46 stations. The observational data used was averaged over the whole measurement period and scaled to an average solar year of solar modulation function Φ=700 MeV (see Koch et al. (1996) for description).

Less data is available in the case of ^{7}Be deposition fluxes, providing, therefore, less than worldwide coverage. The data

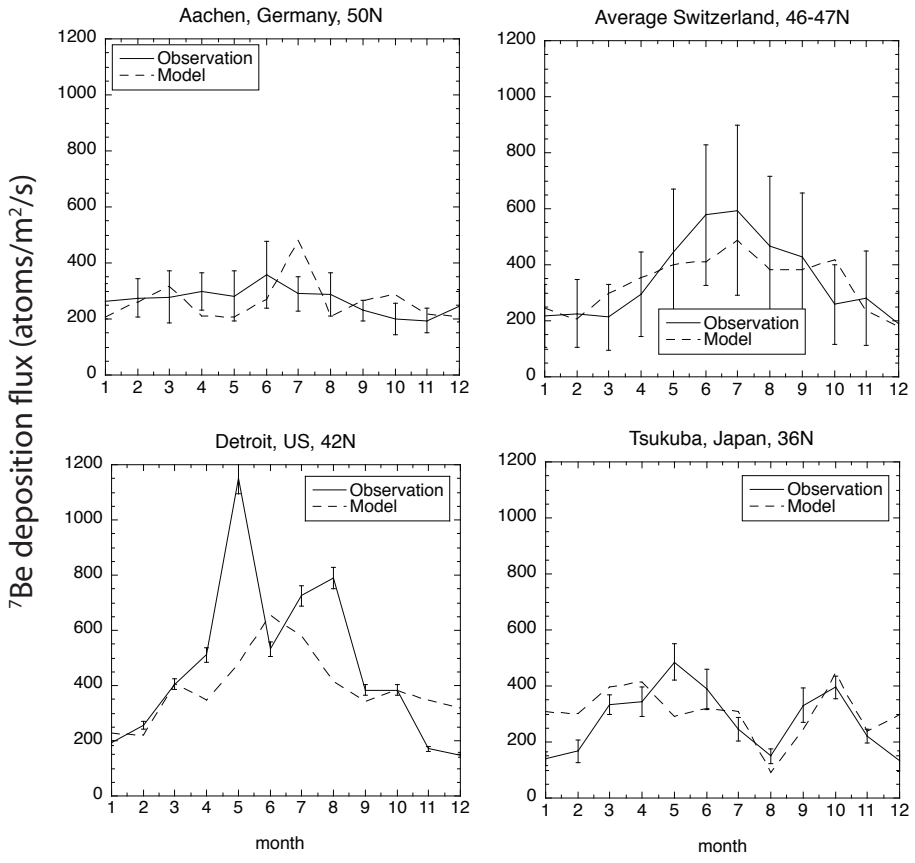

Fig. 4. ^{7}Be seasonal deposition fluxes modeled (dashed line) and observed (full line) in Germany, Switzerland, US and Japan. The error bars show the standard deviations of the annual averages, except at Detroit, where the measurement errors (<5%) are shown. The observational data covers several years, except at Detroit (18 months).

used in this study is from 36 stations and is generally the same as used by Koch et al. (1996) and Land and Feichter (2003).

Figure 2 compares the modeled and measured annual average ^{7}Be concentrations and deposition fluxes from different continents. The ^{7}Be surface air concentrations agree generally within a factor of 2 with the observed concentrations and there seems to be no regional bias. Only at two of the Antarctic stations are the modeled concentrations too low. The agreement of the deposition fluxes is also good although the modeled values deviate more from the observations than the surface air concentrations. This is probably due to the fact that annual variations are less smoothed out during shorter observation times of the deposition fluxes.

The seasonal ^{7}Be surface air concentrations are shown for selected stations in Fig. 3. Overall, the modeled concentrations agree well with the measurements at continental stations and high altitude stations as well as on the islands. Local surface air concentrations are controlled by a multitude of processes including small-scale and large-scale transport processes, precipitation along the transport path, boundary layer turbulence etc. The impact of precipitation at the measurement site on air concentrations is quite small and therefore the good agreement between the modeled and observed concentrations gives confidence to the model's ability to simulate the transport processes well. At Kap Tobin in Greenland the model simulates the correct order of magnitude of the observations but the strong seasonality observed is not reproduced. A similar though less pronounced effect is observed in Antarctica.

Seasonal ^{7}Be deposition fluxes measured in Germany (Thomas Steinkopff, German Weather Service, private communication), Switzerland (Heikkilä et al., 2008a), United States (McNeary and Baskaran, 2003) and Japan (Igarashi et al., 1998) are shown in Fig. 4. The observed seasonal fluxes were averaged over the measurement period, which was usually not the same as the modeled period. At the European and Japanese stations the data cover several years, at Detroit only 18 months, leading to a larger monthly variability. The error bars are standard deviations of the monthly averages. In the case of Detroit the measurement errors are given (<5%).

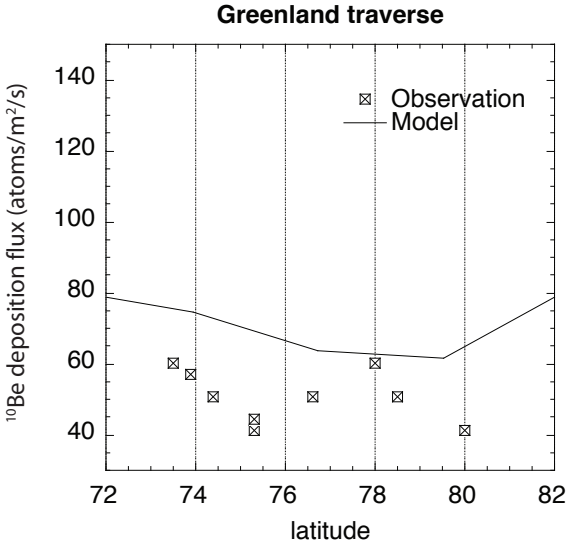

Fig. 5. Comparison of the ^{10}Be deposition flux as a function of latitude averaged over Greenland with observed fluxes during the modeled period of 1986–1990 (Stanzick, 1996).

To validate the modeled ^{10}Be deposition fluxes in Greenland, we compare them with the fluxes measured during a Greenlandic traverse (Stanzick, 1996) from central to northern Greenland. Shallow cores from different latitudes cover periods ranging from medieval times to the mid 1990's (Fig. 5). Only those fluxes are used which coincide with the calculated period. The modeled ^{10}Be deposition flux was averaged over the longitudes of the observations. The agreement between the measured and modeled fluxes is generally good. The observed variability of up to a factor of 1.5 is probably due to the different longitudes at which the cores were taken during the traverse. Since these longitudinal changes are of sub-grid scale the model cannot resolve them. The modeled fluxes are approximately 30 % higher than the observed fluxes, being well within the accepted uncertainty of a factor of two.

A detailed comparison with the modeled and observed ^{10}Be snow concentrations and deposition fluxes as well as precipitation rates in Greenland has been published by Heikkilä et al. (2008b).

3.2 Altitude profiles

In Fig. 6 the modeled ^{10}Be and ^{7}Be concentrations in air are compared with observations from aircraft measurements (Dibb et al., 1997; Jordan et al., 2003; Winiger et al., 1976) from the troposphere and lower stratosphere (altitudes between 0 and 14 km). All observations are from the Northern Hemisphere, representing different longitudes and time periods. Because of their instantaneous character, the observations represent specific meteorological conditions and only provide a range within which the modeled concentrations should lie. Therefore we compare them with modeled zonal mean values of four different latitude bands (30–40° N, 40–50° N, 50–60° N and 60–70° N) corresponding to the observations. If the modeled zonal mean values lie between the range of the observations, we consider the agreement between the modeled and measured concentrations to be good.

In the stratosphere, the concentrations are mostly lower at low latitudes and increase towards the poles in concordance with the latitudinal dependence of the ^{10}Be and ^{7}Be production rates. In the troposphere this structure disappears due to tropospheric transport and precipitation. The variability in the observational data is high, especially at 10–11 km, depending on whether the samples were taken in the stratosphere or in the troposphere, and also on the temporal and longitudinal differences of the observations. The modeled concentrations tend to be on the low side of the observations, especially in the case of ^{10}Be. Too low concentrations in the stratosphere indicate that in the model the tracers are transported downwards too rapidly and therefore cannot accumulate enough. ^{7}Be is less affected by this process than ^{10}Be because of its short half-life compared with the stratospheric residence times. A too strong STE seems to be a common problem of many GCMs, including ECHAM5 and is likely to be associated with too coarse vertical resolution (Timmreck et al., 1999).

4 Comparison between the Maunder Minimum (MM) and the Present Day (PD)

Table 1 shows the global budgets of ^{10}Be and ^{7}Be for the MM and PD simulations. The radionuclide production rate was higher by 32% during MM compared with PD. This leads to a corresponding increase of the ^{10}Be deposition by 32%. In contrast, the ^{7}Be deposition increases by only 20% and the decay by 40%. This means that a larger part of ^{7}Be decays than is deposited, which is due to the larger contribution of stratospheric to total production during the MM. During a period of lower solar activity the contribution of low energy particles to the ^{10}Be and ^{7}Be production is higher (Masarik and Beer, 1999). These particles contribute mostly to the production in the upper atmosphere, which leads to an increased stratospheric fraction of the radionuclide production during MM compared with PD. Figure 7 illustrates the ^{10}Be production change in percent between the MM and PD. The change is largest in the upper atmosphere at high latitudes. This prolongs the atmospheric residence times and increases the burdens by 58% (^{10}Be) and 45% (^{7}Be). The change in the tropospheric burdens of the radionuclides is similar to the deposition change, and the tropospheric residence times remain constant. The fact that the tropospheric residence times are equal in MM and in PD indicates that transport and deposition processes did not change significantly. The ratio of dry to total deposition remains constant.

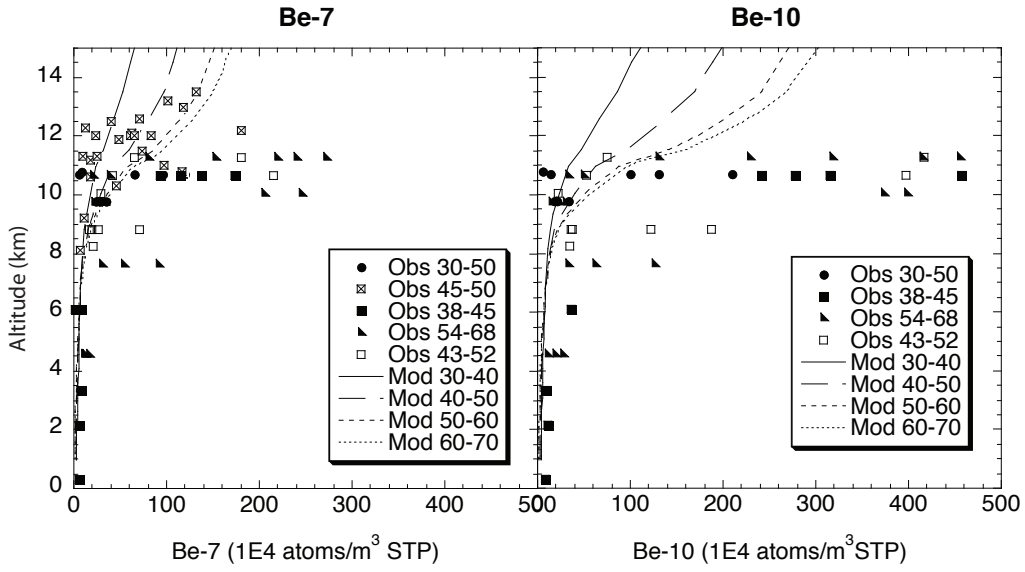

Fig. 6. Zonal mean modeled ^{7}Be (left) and ^{10}Be (right) concentrations in air against altitude for different latitude bands, compared with observations.

Table 1. ^{10}Be and ^{7}Be global averages in Maunder Minimum (MM) and in present day (PD), and change.

^{7}Be	1705–1709	1986–1990	Change MM-PD
Production rate	0.330 g/d	0.252 g/d	31%
Production stratos./tropos.	1.8	1.5	
Wet deposition	0.130 g/d	0.109 g/d	20%
Wet deposition/Dry deposition	92%/8%	93%/7%	
Decay	0.188 g/d	0.134 g/d	40%
Wet deposition/Decay	43% / 57%	47 % / 53 %	
Dry deposition	0.010 g/d	0.008 g/d	
Burden total	14.5 g	10.3 g	41%
Burden stratos.	11.9 g	8.2 g	45%
Burden tropos.	2.5 g	2.1 g	19%
Residence time tropospheric	18 d	18 d	
Residence time total atmosphere	104 d	88 d	18%

^{10}Be	1705–1709	1986–1990	Change MM-PD
Production rate	0.246 g/d	0.186 g/d	32%
Production stratos./tropos.	1.4	1.1	
Wet deposition	0.220 g/d	0.169 g/d	32%
Wet deposition/Dry deposition	92%/8%	92%/8%	
Dry deposition	0.019 g/d	0.014 g/d	
Burden total	42.0 g	27.2 g	54%
Burden stratos.	37.4 g	23.6 g	58%
Burden tropos.	4.6 g	3.6 g	29%
Residence time tropospheric	19 d	20 d	
Residence time total atmosphere	171 d	146 d	17 %

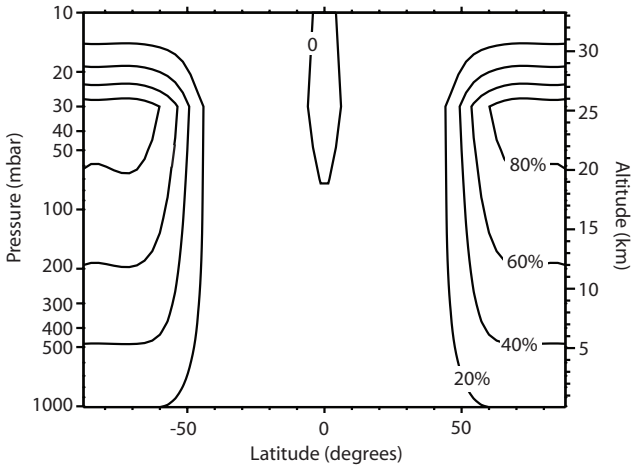

Fig. 7. The production change of ^{10}Be in percent between the Maunder Minimum and the present day (MM-PD).

4.1 Comparison with ice cores

We compare the modeled ^{10}Be concentrations in ice, the deposition fluxes and the precipitation rates with measurements from the two Greenlandic ice cores, Dye3 and Milcent, and two Antarctic ones, the South Pole and Dome Concordia. The comparison of measured and modeled average precipitation rates, ^{10}Be concentrations and fluxes are summarized in Table 2. The precipitation rates are modern values calculated from the accumulation rates measured in the ice cores. The ^{10}Be concentrations are averaged over the period of 1705–1709. The measured fluxes are derived from the measured ^{10}Be concentrations using the modern precipitation rate.

In southern and central Greenland the modeled ^{10}Be concentration in rain during the MM (1.4×10^4 atoms/g) agrees fairly well with the observed concentration ($\sim1.7\times10^4$ atoms/g). At Milcent the modeled precipitation rate (0.8 mm/day water equivalent (W. E.)) is lower than the observed one (1.4 mm/day W. E.). The ^{10}Be flux is also lower than the observed one, but the ^{10}Be concentration in precipitation is correct. If we average over the neighboring grid boxes, the precipitation rate is closer to the observed one (1.0 mm/day W. E.), but the ^{10}Be concentration remains the same. At the Dye3 station the model reproduces the observed precipitation rate well (both 1.4 mm/day W. E.). The ^{10}Be concentration in precipitation (1.2×10^4 atoms/g) also agrees well with the observation (1.5×10^4 atoms/g).

In Antarctica, the precipitation rates are generally lower than in Greenland, leading to higher ^{10}Be concentrations in precipitation. ECHAM5-HAM is capable of simulating the lower precipitation rates in Antarctica, although the precipitation rates at the Antarctic sites are still 2–3 times too high. This leads to a dilution resulting in lower modeled ^{10}Be concentrations in precipitation. Therefore, we also compare the

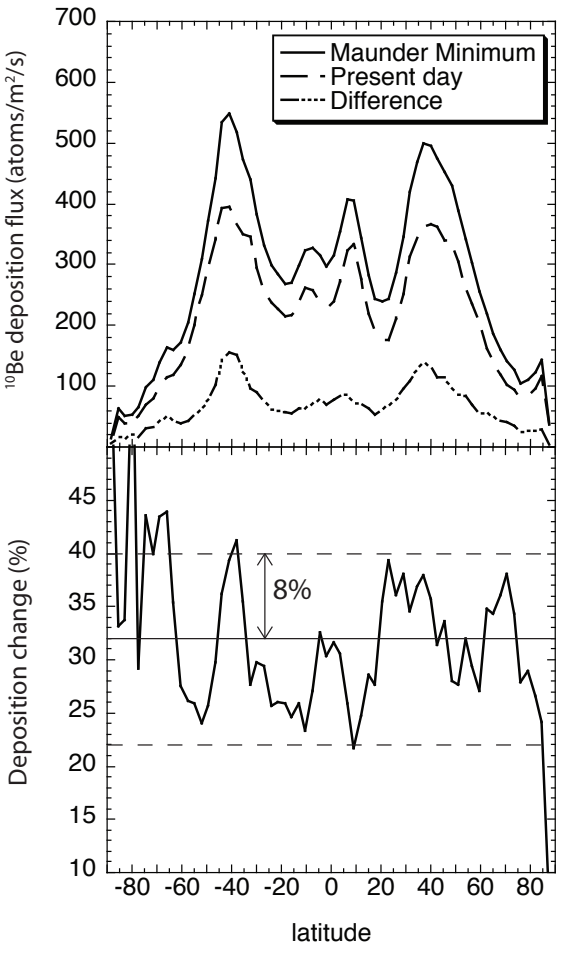

Fig. 8. ^{10}Be zonal mean deposition flux during Maunder Minimum and Present Day, and the change in absolute (atoms/m^2/s, upper panel) and in relative (%, lower panel) units. The zonal mean deposition change is 32±8%. Polewards of 80° the relative difference is higher than this because the deposition fluxes are extremely low in these areas (see upper panel).

deposition fluxes. The observed deposition fluxes in Table 2 are approximated using the modern day precipitation rate because the precipitation rate during the MM is not known. The modeled ^{10}Be deposition fluxes agree within a factor of 2 with the observed fluxes, indicating that the uncertainty is mainly related to an incorrect precipitation rate rather than to transport to the Antarctic continent. This is also confirmed by the good agreement of the modeled ^{7}Be surface air concentrations with the measured data from air filters at the South Pole (see Sect. 3.1).

The precipitation rate modeled at Dome Concordia is approximately 2–3 times too high, leading to a ^{10}Be concentration, which is approximately 6 times too low. The modeled flux is comparable with the observed flux. If we corrected the precipitation rate by a factor of 3, the ^{10}Be concentrations

Table 2. The precipitation rates, given in mm/day Water Equivalent (W. E.), are present day values. The ^{10}Be concentrations and fluxes are averaged over the period of 1705–1709 AD. Measured ^{10}Be fluxes are estimated from the concentrations with the modern day precipitation rate and are only approximations.

Core	Measurement			Model		
	precip. rate (mm/day)	^{10}Be conc. (1E4 at./g)	^{10}Be flux (at./m^2/s)	precip. rate (mm/day)	^{10}Be conc. (1E4 at./g)	^{10}Be flux (at./m^2/s)
Greenland:						
Milcent, 2410 m a.s.l. 70.2° N, 44.4° W	1.4	∼1.7	(∼270)	0.8	1.4	160
Dye 3, 2480 m a.s.l. 65.2° N, 48.8° W	1.4	∼1.5	(∼240)	1.4	1.2	190
Antarctica:						
South Pole, 2800 m a.s.l. 90° S	0.1	∼4	(∼46)	0.2	2.2	61
Dome C, 3240 m a.s.l. 75.1° S, 123.2° E	<0.1	6–7	(∼77)	0.2	1.1	40

would still be too low but within a factor of 2 of the observed value. At the South Pole, the modeled precipitation rate agrees slightly better with the observation than at Dome Concordia, and is twice as high. The ^{10}Be concentration is about a factor of 2 too low and agrees much better with the observations than at Dome Concordia. A correction of the precipitation rate by a factor of 2 would lead to an agreement with the measured ^{10}Be concentration. We conclude that ECHAM5-HAM simulates the ^{10}Be concentrations in Greenland very well, in contrast to Antarctica, where the very low precipitation rates complicate the correct modeling of the concentrations.

The model estimates a rather constant ratio of dry to total deposition (wet and dry) of ^{10}Be in Greenland of approximately 0.9–0.95, which does not vary significantly with latitude. Therefore, changes in precipitation pattern in Greenland should not largely influence the wet/dry deposition ratio. In Antarctica the drier conditions and larger spatial precipitation variability cause the fraction of dry to total deposition to vary more (0.5–0.7). The too high modeled Antarctic precipitation probably leads to somewhat too low fractions of dry to total deposition.

4.2 Change in deposition of ^{10}Be

Figure 8 shows the ^{10}Be deposition fluxes during MM and PD, and the change between the two periods. The distribution of the fluxes is strongly determined by the precipitation rate. The deposition is high in the intertropical convection zone where the precipitation is high, and low in the polar regions with low precipitation. The maximum deposition occurs in the midlatitudes as a result of high precipitation in the midlatitude storm tracks. Moreover, the injections of stratospheric air with high ^{10}Be and ^{7}Be content in the subtropics increase the deposition fluxes broadening the maximum towards these latitudes. Generally the deposition distribution of both ^{10}Be and ^{7}Be (not shown) is very similar, but the ^{10}Be deposition has a larger variability because its changes are not damped by radioactive decay.

Figure 8 also shows the change in ^{10}Be deposition between MM and PD, in absolute and relative units. The absolute change is largest in the subtropics and small in the polar regions. In general, the relative changes are highest in the midlatitudes and in the convection zone. The deviations from the average production-induced change of 32% are within ∼8%. The fact that the production change dominates the variability is an important result because it contradicts the claim that weather-related changes mask the production signal (Lal, 1987). On the other hand, these changes can explain the observed discrepancies between ^{10}Be records from different sites (Fig. 1).

Figures 9 and 10 show the ^{10}Be deposition changes in Greenland and in Antarctica. The absolute deposition change is largest in southern Greenland and decreases towards the pole. The relative change in Greenland seems to follow the topography and is largest at the highest point of Greenland. Both sites, Milcent (2410 m a.s.l.) and Dye3 (2480 m a.s.l.), have the same altitude. The model results reveal similar deposition changes between MM and PD for both sites. In Antarctica, the modeled ^{10}Be concentrations do not agree as well with the observations as in Greenland, but the model uncertainty may be similar for both runs. In Antarctica the change, both absolute and relative, seems to be larger in eastern Antarctica, where Dome Concordia is located, than at the South Pole. This suggests that the change at Dome Concordia was larger than at the South Pole although the accumulation rate at Dome Concordia is smaller. This finding seems to be in agreement with the observed maxima (Fig. 1) during the MM.

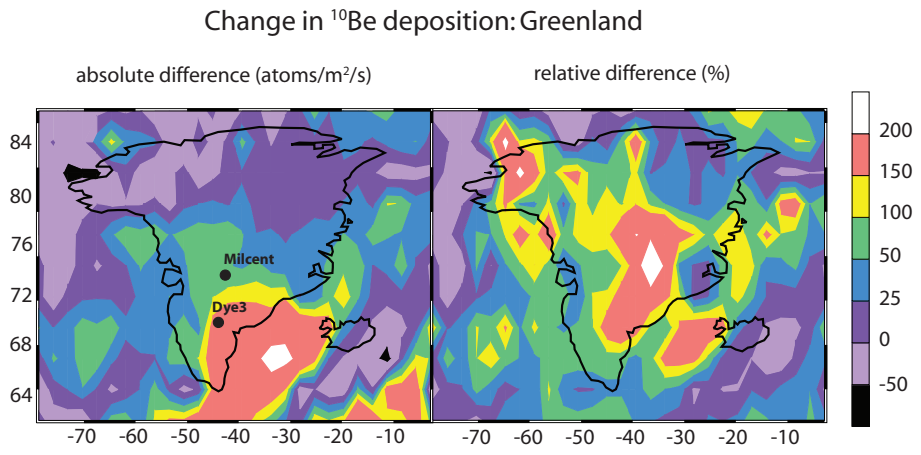

Fig. 9. The change of modeled ^{10}Be deposition between Maunder Minimum and Present Day in Greenland in absolute (atoms/m^2/s, left) and relative (%, right) units

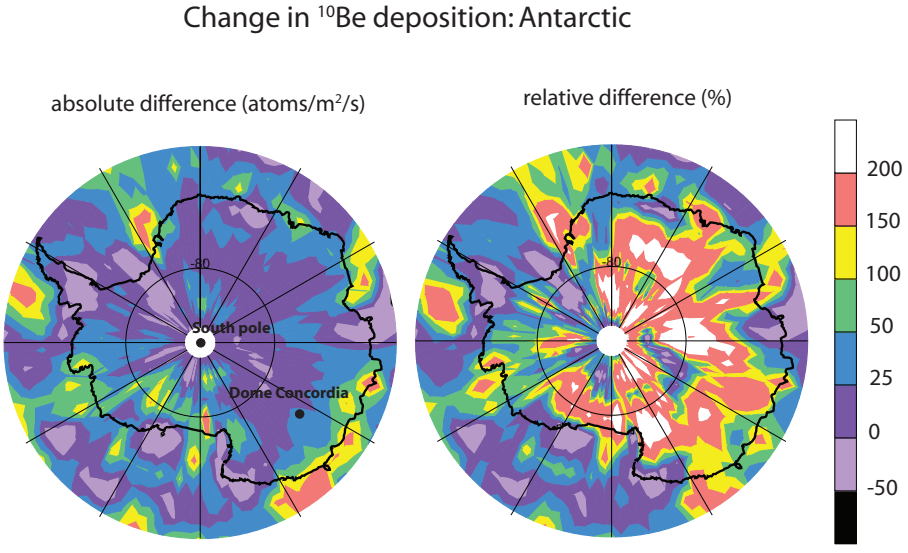

Fig. 10. The change of modeled ^{10}Be deposition between Maunder Minimum and Present Day in Antarctica in absolute (left) and relative (right) units.

4.3 Changes in STE between the Maunder Minimum and the Present Day using ^{10}Be/^{7}Be

To study possible changes in STE between MM and PD, we investigate the ^{10}Be/^{7}Be ratio. At the time of production the global mean ratio is 0.5, but it grows exponentially with time as ^{7}Be decays. In the stratosphere high ratios are observed because of the long residence time which allows ^{7}Be to decay, raising the ratio. In the troposphere the ratios remain closer to 0.5 because the tropospheric residence time is short compared with the half-life of ^{7}Be. Therefore, large ^{10}Be/^{7}Be ratios in the troposphere point to an intrusion of stratospheric air into the troposphere. As the net mass downward flux from the stratosphere shows a distinct seasonal cycle with a maximum in spring in the Northern Hemisphere and in midwinter in the Southern Hemisphere (Stohl et al., 2003), we expect larger ^{10}Be/^{7}Be ratios during these seasons. The upper panel of Fig. 11 shows the zonally averaged seasonal ^{10}Be/^{7}Be ratios calculated from the deposition fluxes.

The slightly higher level of ^{10}Be/^{7}Be ratios during MM is caused by a longer stratospheric residence times of ^{7}Be and ^{10}Be compared with PD, caused by a higher fraction of stratospheric production. Because the increase is similar in all latitudes, it is probably not caused by changes in STE, which has a latitudinal dependence. Instead, because the stratospheric downward fluxes are strongest in

the subtropics, changes in ^{10}Be/^{7}Be ratios at these latitudes could be attributed to STE changes. The lower panel of Fig. 11 shows the relative seasonal change in the ^{10}Be/^{7}Be ratio. The largest change takes place during spring in the Northern Hemisphere at mid- and low latitudes. During the summer months in both hemispheres the ratios are higher than during the winter months probably because of a lower precipitation rate, which increases the tropospheric residence time. During the southern hemispheric fall the ratio has a mid- and low latitude maximum, but it is much less pronounced than in the Northern Hemisphere. These results point to a stronger STE in the Northern Hemisphere during the colder climate of MM. In the Southern Hemisphere the changes were probably not significant.

5 Summary and conclusions

The cosmogenic radionuclides ^{10}Be (half-life 1.5×10^{6} years) and ^{7}Be (half-life 53.2 days) have been modeled during the Maunder Minimum (MM) and the present day (PD) climate with the ECHAM5-HAM general circulation model. We concentrated on changes which can influence the ^{10}Be concentrations measured in ice cores such as enhanced radionuclide production, possible changes in the stratosphere-troposphere exchange (STE), and in the local precipitation rate at the measurement sites. We also investigated to what extent climate changes during a period of low solar activity mask the production signal in the measured ^{10}Be concentrations in ice cores.

The lower solar activity during the MM raises the mean global production rate of ^{10}Be and ^{7}Be by 32%. Moreover, the production becomes stronger in the upper atmosphere, raising the ratio of stratospheric to total production. This leads to longer atmospheric residence times and higher stratospheric burdens of the radionuclides. Higher stratospheric burdens cause a higher radionuclide content in the downward fluxes from the stratosphere. This causes higher deposition fluxes during MM in the subtropics, but in the polar regions the effect is small.

While the total ^{10}Be deposition increases by 32%, directly reflecting the increase in production rate, the ^{7}Be deposition increases only by 20% because a larger part of ^{7}Be decays due to longer atmospheric residence times. The zonal mean ^{10}Be deposition change deviates locally only by ∼8% from the mean increase of 32%. The ∼8% variation represents the climate signal, which is caused by changes in precipitation rate and tropospheric transport. It is small compared to the production change. Therefore, the common assumption made so far when reconstructing the solar activity, namely that the ^{10}Be measured in ice is proportional to the total production rate, seems reasonable.

It has to be kept in mind that the uncertainly of the solar forcing during the Maunder Minimum is large, as well as the climate response to the forcing. We are not able to validate

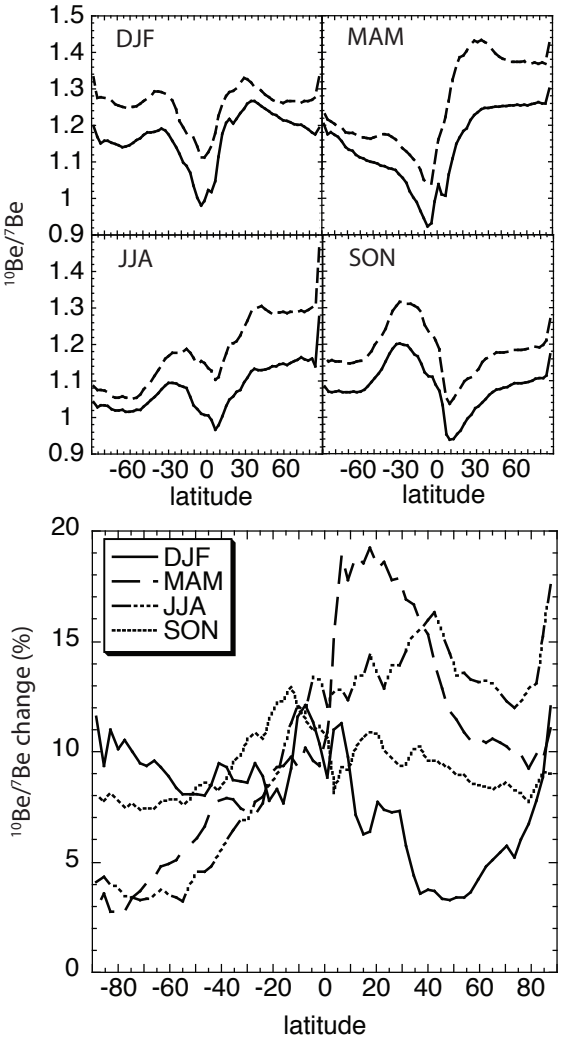

Fig. 11. The seasonal ^{10}Be/^{7}Be ratio of the deposition fluxes (Maunder Minimum: dashed line, Present day: full line), and the difference between Maunder Minimum and Present day in %.

the simulated temperature or precipitation rates during the Maunder Minimum, we can only compare them with other estimates. However, the main result of this study namely that the ^{10}Be deposition is mostly determined by its production rate even in a significantly cooler climate is still valid, although the generation of the cooler climate might include some uncertainty.

The ECHAM5-HAM simulates the ^{10}Be fluxes and concentrations in ice at Greenlandic sites fairly well. In Antarctica the model has some difficulties in reproducing the very low level of precipitation which leads to an underestimation of the ^{10}Be concentrations in ice. In Greenland the absolute deposition change between MM and PD seems to depend on the topography with a north-south gradient and with the largest values in the south of Greenland. The relative difference is largest at high altitudes. The model results suggest

a similar deposition change between MM and PD at Dye3 and Milcent. In Antarctica the modeled deposition changes remain generally small, especially in dry areas. The model results suggest that the change was larger at Dome Concordia than at the South Pole.

Finally, the ^{10}Be/^{7}Be ratio is generally higher due to a longer stratospheric residence time during the MM. This longer residence time is primarily the result of a change in the structure of stratospheric to tropospheric production between MM and PD and not in the STE. However, during spring in the Northern Hemisphere a large increase in the ratio between the 20° N and 40° N is observed, which probably can be attributed to a stronger STE during the MM. In the Southern Hemisphere no such strong change was observed.

These findings compare generally well with the results of Field et al. (2006). They investigated the separate contribution of different production or climate related factors which influence the deposition fluxes of ^{10}Be in polar regions. Because the present experiment combines both production and climate change our results cannot be compared quantitatively with the results of Field et al. (2006). However, their major conclusions that the ^{10}Be response to climate should not be neglected when inferring production changes and that the production variability inferred from polar ^{10}Be fluxes might overestimate the global production variability are in good agreement with our results. We find that although the climate induced changes of the ^{10}Be fluxes are considerably smaller than the production induced changes, they cannot be neglected. Due to these climate-induced fluctuations the variability of polar ^{10}Be fluxes is probably larger than the variability of the global production rate.

Both the model experiment as well as the good agreement between ^{10}Be in ice cores and ^{14}C in tree rings point to a dominant production signal which confirms the suitability of ^{10}Be for reconstructing the solar activity. Modeling the atmospheric transport improves the interpretation of ^{10}Be in ice cores in terms of production effects and helps to make full use of cosmogenic radionuclides. At the same time atmospheric ^{10}Be and ^{7}Be data provide a tool to study atmospheric transport processes such as the STE, and to validate GCMs.

Acknowledgements. We are grateful to the German Computer Center (DKRZ) for providing us with the computing time. This work is financially supported by the Swiss National Science Foundation.

Edited by: K. Carslaw

References

Bard, E., Raisbeck, G., Yiou, F., and Jouzel, J.: Solar modulation of cosmogenic nuclide production over the last millennium: comparison between ^{14}C and ^{10}Be records, Earth. Plan. Sci. Lett., 150, 453–462, 1997.

Baskaran, M., Coleman, C., and Santchi, P.: Atmospheric depositional fluxes of ^{7}Be and ^{210}Pb at Galveston and College Station, Texas, J. Geophys. Res., 98, 20 555–20 571, 1993.

Beer, J., Siegenthaler, U., and Blinov, A.: Temporal ^{10}Be variations in ice: Information on solar activity and geomagnetic field intensity, in: Secular Solar and Geomagnetic Variations in the Last 10,000 Years, Kluwer Academic Publishers, 297–313, 1988.

Beer, J., Siegenthaler, U., Bonani, G., Finkel, R., Oeschger, H., Suter, M., and Wölfli, W.: Information on past solar activity and geomagnetism from ^{10}Be in the Camp Century ice core, Nature, 331, 6158, 675–679, 1988.

Beer, J., Blinov, A., Bonani, G., Finkel, R. C., Hofmann, H. J., Lehmann, B., Oeschger, H., Sigg, A., Schwander, J., Staffelbach, T., Stauffer, B., Suter, M., and Wölfli, W.: Use of ^{10}Be in polar ice to tracer the 11-year cycle of solar activity, Letters to Nature, 347, 164–166, 1990.

Beer, J., Baumgartner, S., Dittrich-Hannen, B., Hauenstein, J., Kubik, P., Lukasczyk, C., Mende, W., Stellmacher, R., and Suter, M.: Solar variability traced by cosmogenic isotopes in the Sun as a variable star: Solar and stellar irradiance variations, edited by: Pap, J. M., Fröhlich, C., Hudson, H. S., and Solanki, S. K., Cambridge University Press, 291–300, 1994.

Brown, L., Stensland, G.J., Klein, J., and Middleton, R.: Atmospheric deposition of ^{7}Be and ^{10}Be, Geochim. Cosmochim. Ac., 53, 135–142, 1988.

Crowley, T.: Causes of Climate Change Over the Past 1000 Years, Science, 289, 270–277, 2000.

Dibb, J. E., Talbot, R. W., Lefer, B. L., Scheuer, E., Gregory, G. L., Browell, E. V., Bradshaw, J. D., Sandholm, S. T., and Singh, H. B.: Distributions of beryllium 7 and lead 210, and soluble aerosol-associated ionic species over the western Pacific: PEM West B, February–March 1994, J. Geophys. Res., 102, 28 287–28 302, 1997.

Feichter, J., Roeckner, E., Lohmann, U., and Liepert, B.: Nonlinear aspects of the climate response to greenhouse gas and aerosol forcing, J. Climate, 17, 12, 2384–2398, 2004.

Field, C., Schmidt, G., Koch, D., and Salyk, C.: Modeling production and climate-related impacts on ^{10}Be concentration in ice cores, J. Geophys. Res., 111, D15107, doi:10.1029/2005JD00640, 2006.

Gonzalez-Rouco, J. F., Zorita, E., Cubasch, U., von Storch, H., Fischer-Bruns, I., Valero, F., Montavez, J. P., Schlese, U., and Legutke, S.: Simulating the climate since 1000 AD with the AOGCM ECHO-G, in: Proceedings of the ISCS1 2003 symposium Solar Variability as an Input to the Earth's Environment, Tatranská Lomnica, Slovakia, 23–28 June 2003, ESA SP-535, 329–338, 2003.

Graham, I., Ditchburn, R., and Barry, B.: Atmospheric deposition of ^{7}Be and ^{10}Be in New Zealand rain (1996–1998), Geochim. Cosmochim. Ac., 67, 361–373, 2003.

Heikkilä, U., Beer, J., and Alfimov, V.: ^{10}Be and ^{7}Be in precipitation in Dübendorf (440 m) and at Jungfraujoch (3580 m), Switzerland (1998–2005), J. Geophys. Res., doi:10.1029/2007JD009160, in press, 2008a.

Heikkilä, U., Beer, J., Jouzel, J., Feichter, J., and Kubik, P.: ^{10}Be measured in a GRIP snow pit and modeled using the ECHAM5-HAM general circulation model, J. Geophys. Res., 35, L05817 doi:10.1029/2007GL033067, 2008b.

Igarashi, Y., Hirose, K., and Otsuji-Hatori, M.: Beryllium-7 deposition and its relation to sulfate deposition, J. Atmos. Chem., 29, 217–231, 1998.

Jordan, C. E., Dibb, J. E., and Finkel, R. C.: ^{10}Be/^{7}Be tracer of atmospheric transport and stratosphere–troposphere exchange, J. Geophys. Res., 108(D8), 4234, doi:10.1029/2002JD002395, 2003.

Koch, D., Jacob, D., and Graustein, W.: Vertical transport of tropospheric aerosols as indicated by ^{7}Be and ^{210}Pb in a chemical tracer model, J. Geophys. Res., 101, 18 651–18 666, 1996.

Koch, D. and Rind, D.: Beryllium-10/Beryllium-7 as a tracer of stratospheric transport, J. Geophys. Res., 103, 3907–3917, 1998.

Kolb, W.: Aktivitätskonzentrationen von Radionukliden in der bodennahen Luft Norddeutschlands und Nordnorwegens im Zeitraum von 1963 bis 1990, Report PTB-Ra-29, Physikalisch Technische Bundesanstalt, Braunschweig, Germany, 129 pp., 1992.

Kollár, D., Leya, I., Masarik, J., and Michel, R.: Calculation of cosmogenic nuclide production rates in Earth's atmosphere and in terrestial surface rocks using improved neutron cross sections, Meteoritics, 35, A90–A91, 2000.

Lal, D. and Peters, B.: Cosmic ray produced radioactivity on the Earth, Handbuch der Physik, XLVI/2, Springer-Verlag, New York, 551–612, 1967.

Lal, D.: ^{10}Be in polar ice: Data reflect changes in cosmic ray flux or polar meteorology, Geophys. Res. Lett., 14, 785–788, 1987.

Land, C. and Feichter, J.: Stratosphere-troposphere exchange in a changing climate simulated with the general circulation model MAECHAM4, J. Geophys. Res., 108(D12), 8523, doi:10.1029/2002JD002543, 2003.

Langematz, U., Claussnitzer, A., Matthes, K., and Kunze, M.: The climate during the Maunder Minimum: a simulation with the Freie Universität Berlin Climate Middle Atmosphere Model (FUB-CMAM), J. Atmos. Sol.-Terr. Phy., 67, 55–60, 2005.

Luterbacher, J.: Climate reconstruction and synoptic analysis of the Late Maunder Minimum (AD 1675–1715) period, PhD Thesis, University of Bern, 1999.

Masarik, J. and Beer, J.: Simulation of particle fluxes and cosmogenic nuclide production in the Earth's atmosphere, J. Geophys. Res., 104, 12 099–12 111, 1999.

McCracken, K., McDonald, F., Beer, J., Raisbeck, G., and Yiou, F.: A phenomenological study of the long–term cosmic ray modulation, 850–1958 AD, J. Geophys. Res., 109, A12103, doi:1029/2005JA10685, 2004.

McNeary, D. and Baskaran, M.: Depositional charasteristics of ^{7}Be and ^{210}Pb in southeastern Michigan, J. Geophys. Res., 108(D7), 4210, doi:10.1029/2002JD00321, 2003.

Monaghan, M. C., Krishnaswami, S., and Turekian, K. K.: The global-average production of ^{10}Be, Earth Planet. Sci. Lett., 76, 279–287, 1985/1986.

Muscheler, R., Joos, F., Beer, J., Müller S, Vonmoos, M., and Snowball, I.: Solar activity during the last 1000 yr inferred from radionuclide records, Quarternary Sci. Rev., 26, 82–97, 2007.

Raisbeck, G. M., Yiou, F., Fruneau, M., Lieuvin, M., and Loiseaux, J. M.: Measurement of ^{10}Be in 1,000– and 5,000–year–old Antarctic ice, Nature, 275, 731–733, 1978.

Raisbeck, G. M., Yiou, F., Jouzel, J., and Petit, J. R.: ^{10}Be and δ^{2}H in polar ice cores as a probe of solar variability's influence on climate, Phil. Trans. R. Soc. Lond. A, 330, 463–470, 1990.

Rehfeld, S. and Heimann, M.: Three dimensional atmospheric transport simulation of the radioactive tracers ^{210}Pb, ^{7}Be, ^{10}Be and ^{90}Sr, J. Geophys. Res., 100, 26 141–26 161, 1995.

Roeckner, E., Baeuml, G., Bonventura, L., Brokopf, R., Esch, M., Giorgetta, M., Hagemann, S., Kirchner, I., Kornblueh, L., Manzini, E., Rhodin, A., Schlese, U., Schulzweida, U., and Tompkins, A.: The atmospheric general circulation model ECHAM5, PART I: Model description, Report 349, Max Planck Institute for Meteorology, Hamburg, Germany, available from: http://www.mpimet.mpg.de, 2003.

Stanzick, A.: Räumliche und zeitliche Depositionsvariationen der Radioisotope ^{10}Be und ^{210}Pb in Eisbohrkernen Zentralgrönlands, Diploma thesis, University of Heidelberg, 1996.

Stier, P., Feichter, J., Kinne, S., Kloster, S., Vignati, E., Wilson, J., Ganzeveld., L., Tegen, I., Werner, M., Schulz, M., Balkanski, Y., Boucher, O., Minikin, A., and Petzold, A.: The aerosol-climate model ECHAM5-HAM, Atmos. Chem. Phys., 5, 1125–1165, 2005, http://www.atmos-chem-phys.net/5/1125/2005/.

Stohl, A., Bonasoni, P., Cristofanelli, P., Collins, W., Feichter, J., Frank, A., Forster, C., Gerasopoulos, E., Gäggeler, H., James, P., Kentarchos, T., Kromp-Kolb, H., Krüger, B., Land, C., Meloen, J., Papayannis, A., Priller, A., Seibert, P., Sprenger, M., Roelofs, G. J., Scheel, H. E., Schnabel, C., Siegmund, P., Tobler, L., Trickl, T., Wernli, H., Wirth, V., Zanis, P., and Zerefos, C.: Stratosphere-troposphere exchange: A review, and what we have learnt from STACCATO, J. Geophys. Res., 108(D12), 8516, doi:10.1029/2002JD002490, 2003.

Timmreck, C., Graf, H.-F., and Feichter, J.: Simulation of Mt. Pinatubo volcanic aerosol with the Hamburg Climate Model ECHAM4, Theor. Appl. Climatol., 62, 85–108, 1999.

Usoskin, I. G., Alanko-Huotari, K., Kovaltsov, G. A., and Mursula, K.: Heliospheric modulation of cosmic rays: Monthly reconstruction of 1951–2004, J. Geophys. Res., 110, A12108, doi:10.1029/2005JA011250, 2005.

Vonmoos, M., Beer, J., and Muscheler, R.: Large variations in Holocene solar activity: Constraints from ^{10}Be in the Greenland Ice Core Project ice core, J. Geophys. Res., 111, A10105, doi:10.1029/2005JA011500, 2006.

Winiger, P., Huber, O., Halter, J., and Michaud, B.: Konzentrationsmessungen von Be-7, Cs-137 und jungen Spaltfragmenten an der Tropopause, Tellus, 28, 434–441, 1976.

Yang, S., Odah, H., and Shaw, J.: Variations in the geomagnetic dipole moment over the last 12 000 years, Geophys. J. Int., 140, 158–162, 2000.

Zorita, E., Gonzalez-Rouco, J. F., von Storch, H., Montavez, J. P., and Valero, F.: Natural and anthropogenic model of surface temperature variations in the last thousand years, J. Geophys. Res., 32, L08707, doi:10.1029/2004GL021563, 2005.